

Numerical simulation of turbulence flow in a Bulb turbine

Yasuyuki ENOMOTO¹, Takanori NAKAMURA², Norio OHTAKE³,
Koichi KUBO⁴, Yabin ZHAI⁵

^{1,2,3,4,5} Toshiba Corporation
20-1 Kansei-cho, Tsurumi-ku, Yokohama, 230-0034, Japan

E-mail : yasuyuki.enomoto@toshiba.co.jp

Abstract. In this paper, high accuracy performance prediction method based on entire flow passage for a Bulb turbine is presented. The performance is predicted by solving steady and unsteady Reynolds-Averaged Navier-Stokes equations, Large Eddy simulation and Detached Eddy Simulation. The prediction accuracy was evaluated to compare with the model test results for efficiency characteristic, pressure fluctuation characteristic and velocity distribution at runner inlet and outlet of N_{QE} 0.8 Bulb model turbine. As for the efficiency near the on-cam condition, it is possible to determine with high accuracy in the steady RANS analysis. However, for the analysis accuracy regarding pressure fluctuation characteristic and turbine characteristics at off-cam operating condition, it found that there is a need to further study. Evaluated prediction method for the turbine flow and performance is introduced to facilitate the future design and research works on Bulb type turbine.

1. Introduction

Hydroelectric power generation is one of the environment-friendly power generation systems compared with existent electric power generating equipment and extremely outstanding renewable energy. The kinds of hydro turbine are Francis turbine, Kaplan turbine, Bulb turbine, Pelton turbine and so on. In particular, Bulb turbines are used in the area with the low head places. The demands for high performance Bulb turbine which has high efficiency and low pressure fluctuation characteristics have been increasing in recent years. In order to develop high performance hydro turbine, many designers use various design optimization techniques [1, 2, 3]. In their optimization stage, flow analysis is used often. The accuracy of flow analysis will affect the optimization result, the flow analysis accuracy is very important. For the accuracy of flow analysis for the hydro turbine, a lot of research results have been reported. In general, the turbulent flow analysis is used in the flow analysis of the hydro turbine. Reynolds-Averaged Navier-Stokes (RANS) equations and Large Eddy Simulation (LES) are often used. As for the RANS, turbine efficiency and occurrence of cavitation were accurately predicted by using Reynolds-Stress Model (RSM) for Francis turbine [4] and for the Kaplan turbine [5]. Regarding Large Eddy Simulation, accurate for predicting the flow in draft tube was reported [6]. However, such analysis technique takes a long analysis time for the large number of meshes required. Therefore, it is not appropriate to be used for the hydro turbine shape design optimization for many calculations. In this paper, the effect of turbulence models and boundary conditions influence on the analysis accuracy was investigated for a specific speed N_{QE} 0.8 Bulb model turbine. The performance is predicted by solving steady and unsteady Reynolds-Averaged Navier-Stokes (RANS and URANS) equations, Large Eddy Simulation and Detached Eddy Simulation (DES). The prediction accuracy was evaluated to compare with the model test results



which include turbine efficiency, velocity distribution and pressure fluctuation. Evaluated prediction method for the turbine flow and performance is introduced to facilitate the future design and research works on Bulb type turbine.

2. Prediction method of model turbine performance

2.1. Fundamental formulations and physical model

The fundamental formulations for the performance characteristics of a Bulb turbine are given as follows.

$$H_M = H_1 - H_2 \quad (1)$$

$$H_{th} = \frac{2\pi \times n_M \times T_M}{60 \times Q_{IM}} \quad (2)$$

$$\eta_{hM} = \frac{H_{th}}{H_M} \quad (3)$$

$$n_{ED} = \frac{n_M \cdot D_M}{\sqrt{H_M \cdot g_M}} \quad (4)$$

$$Q_{ED} = \frac{Q_{IM}}{D_M^2 \cdot \sqrt{H_M \cdot g_M}} \quad (5)$$

Q_{IM} , n_M , H_M , T_M , D_M , g_M are discharge, rotational speed, turbine head, runner torque, diameter of runner and gravity acceleration respectively. H_M is calculated by using the total pressure difference between turbine inlet (H_1) and turbine outlet (H_2). H_{th} is the theoretical head acting on runner blades and is represented by eq.(2).

Turbine efficiency (η_{hM}) is predicted by dividing theoretical head with the turbine head. The prediction of the turbine performance in the operating range is done by the use of speed factor and discharge factor, which are derived from given actual rotational speed, discharge, and predicted turbine head.

2.2. Numerical method

Commercial CFD software “ANSYS CFX” 14.5 is used. In this paper, 4 calculations shown below were conducted.

- 1) Reynolds-Averaged Navier-Stokes calculation
- 2) Unsteady Reynolds-Averaged Navier-Stokes calculation
- 3) Large Eddy Simulation
- 4) Detached Eddy Simulation

Today, most CFD simulations are carried out with traditional Reynolds-Averaged Navier-Stokes (RANS). In RANS, various turbulence models are existed such as k-epsilon, k-omega, SST, Reynolds Stress Model and so on. In this paper, SST turbulence model is applied.

LES calculation is mainly used in unsteady flow with wake flow or with large separation flow. In this paper LES smagorinsky model is applied.

In order to extend LES to high Reynolds number flows, new methods such as Detached Eddy Simulation (DES), Partially Integrated Transport Model and Partially Averaged Navier-Stokes have recently been developed. DES is hybrid model of LES and RANS, RANS is used near wall surface. In this paper, DES was used in unsteady calculation.

2.3. Computational grid and boundary condition

In this paper, N_{QE} 0.8 bulb model turbine is studied. Bulb turbine is used in wide operating range. Therefore, the efficiency and pressure fluctuation at large discharge condition not only design point are also important. In this calculation, the accuracy at the large discharge condition is examined. The

guide vane angle is set about 1.2 times at design condition and the runner blade angle is set about 1.7 times in design condition. Configuration and summary of this turbine is shown in Figure 1 and Table 1. The calculation conditions are summarised in Table 2.

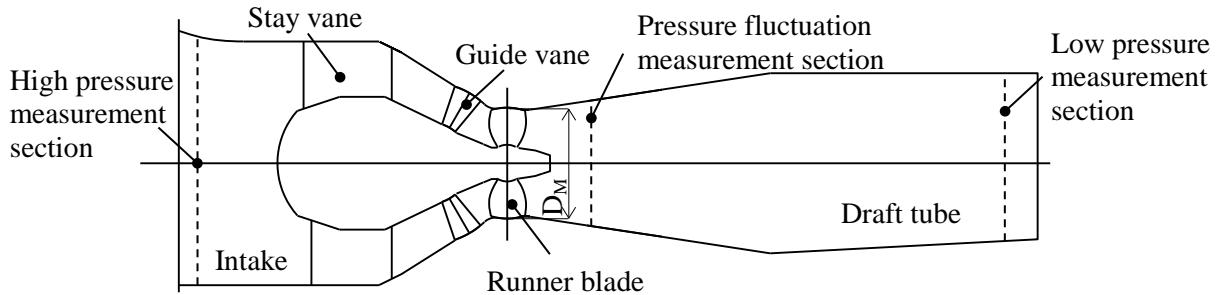


Figure 1. Configuration of N_{QE} 0.8 Bulb model turbine

Table 1. Principal dimension of Bulb model turbine

Runner outlet diameter	D_M	350 mm
Stay vane number	Z_s	2
Guide vane number	Z_g	16
Runner blade number	Z_r	3

Table 2. Calculation conditions

Speed factor	1.1~1.6
Runner blade angle	25deg (opening direction)
Guide vane angle	68.3deg (opening direction)

The computational model is shown in Figure 2. In this calculation, in order to compare the flow including the influence of upstream and downstream of model bulb turbine, head tank and suction tank in addition to bulb turbine are also modelled. The number of grid points is about 16 million. In the numerical simulation, it adopts the high order numerical scheme and the high accuracy turbulence model. Therefore higher grid quality needs to be kept as well to avoid the instability in the calculation. The computational boundary conditions are applied at the inlet surface and at the outlet surface of the computational domain. About the inlet boundary condition, a uniform velocity distribution is assumed. As for the outlet boundary condition, the average pressure is set to fix. Furthermore, about the surface of the passage wall, the non-slip boundary condition is prescribed, i.e. the velocity components are set to zero. At inter faces at rotational part and stationary part, two conditions are applied. One is a Frozen rotor inter face condition and another is a Stage inter face condition applying circumferential direction mean value.

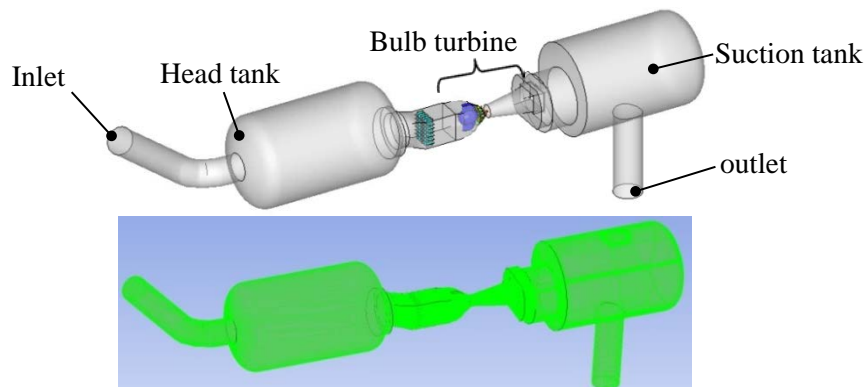


Figure 2. Overview of computational model

3. Experiment

Validation data for numerical results are measured on a test rig at Hydraulic research laboratory in Toshiba Corporation. The test rig for model turbine is shown in Figure 3 as a typical example. The model test was conducted on the basis of IEC standard. The turbine efficiency and pressure fluctuation at runner outlet are measured. Besides turbine characteristic, velocity distribution at intake, guide vane outlet and draft tube were measured by Laser Doppler Velocimetry (LDV).

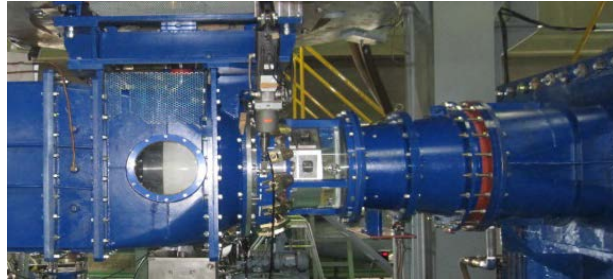


Figure 3. Model test equipment for Model hydro turbine

4. Simulation results and discussion

4.1. Model turbine efficiency

Figure 4 shows the comparison of the relative efficiency (η_{hM}/η_{hM0}) which is normalized model maximum efficiency (η_{hM0}) in tested guide vane angle and runner blade angle condition. In this figure, red line shows model test results (Experiment), and others show CFD results. Steady calculation was performed in two cases with different boundary conditions. One is applied Frozen Rotor inter face (Frozen rotor), and another is applied Stage inter face (Stage). And unsteady calculations were performed in three cases with different calculation method. First one is used URANS calculation with SST turbulent model (SST), second one is DES (DES) and third one is LES (LES). All these calculations were performed using the same computational grids. At this guide vane angle and runner blade angle condition, around 1.2 speed factor (n_{ED}) condition is on-cam condition. Around on-cam operating condition, predicted efficiency by CFD is relatively close to model test results except LES result. However off-cam condition such as high speed factor operating condition, the difference between model test results and prediction results by CFD become large.

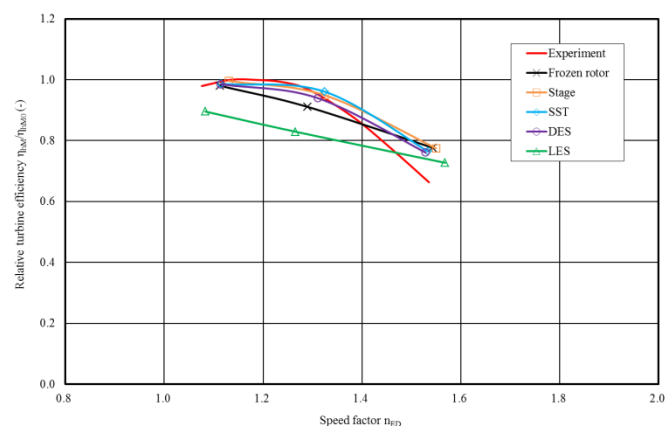


Figure 4. The comparison of efficiency between the numerical and experimental results

Figure 5 shows hydraulic losses calculated by CFD at each component near 1.1 speed factor condition. The each component losses are defined by following formulation.

$$\begin{aligned} \text{Stay vane loss} & : \text{Loss}_{sv} = H_1 - H_{gv_inlet} \\ \text{Guide vane loss} & : \text{Loss}_{gv} = H_{gv_inlet} - H_{gv_outlet} \\ \text{Runner vane loss} & : \text{Loss}_{rv} = (H_{gv_outlet} - H_{rv_outlet}) - H_{th} \\ \text{Draft tube loss} & : \text{Loss}_{dr} = H_{rv_outlet} - H_2 \end{aligned}$$

where, H_{gv_inlet} : total pressure at guide vane inlet
 H_{gv_outlet} : total pressure at guide vane outlet
 H_{rv_outlet} : total pressure at runner blade outlet

In this figure, each component loss are normalized each component loss calculated by steady calculation with Frozen rotor interface condition. From this figure, the loss varies depending on the analysis method, in particular the difference in draft tube loss is large.

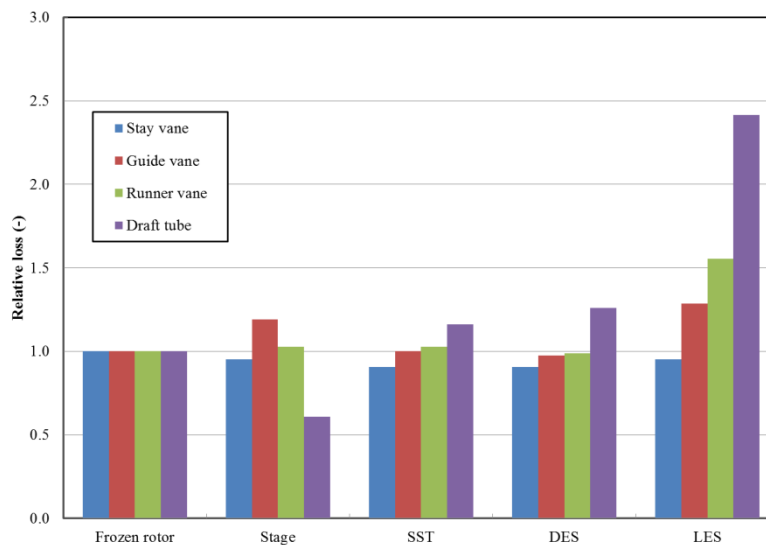


Figure 5. The comparison of hydraulic loss between the numerical and experimental results

Figure 6 shows relative turbine efficiency and relative loss in draft tube. These values are normalized the values of model test results. The operating condition is near 1.1 speed factor condition. At the model test, wall pressure at runner blade outlet and draft tube outlet were measured. Beside the wall pressure, velocity distribution at runner blade outlet was measured. Total pressure at runner outlet was estimated using the dynamic pressure calculated using velocity distribution and the static pressure calculated using wall pressure and velocity distribution. And a total pressure at draft tube outlet was estimated using wall pressure and uniform velocity distribution. By using these total pressures, a draft tube loss can be calculated. It is found from this figure that the draft tube loss predicted by CFD is large compared to the model test result. Especially the loss predicted by LES becomes more than twice the model test results. As a result, predicted efficiency by LES become low compared to model test results.

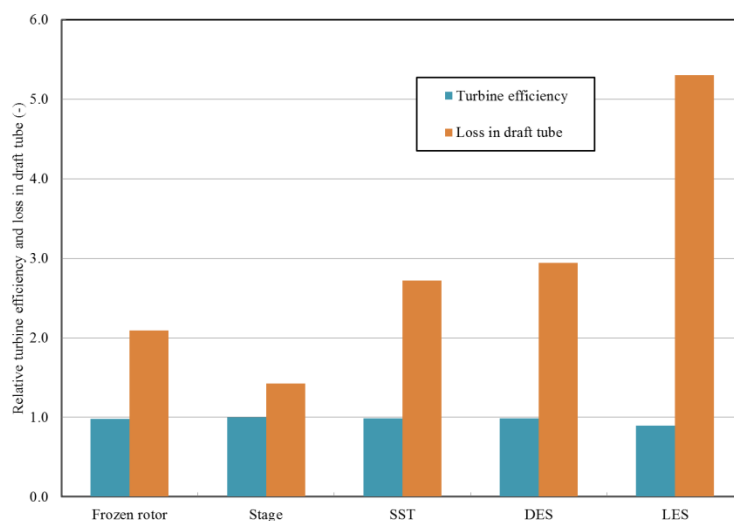


Figure 6. The comparison of efficiency and draft tube loss between the numerical and experimental results

Figure 7 shows the velocity contours at three sections. And Figure 8 to Figure 10 show the flow velocity distributions numerically simulated and experimentally measured. For the unsteady calculation, time averaged velocity are used. In these figures, the velocity value is normalized by the averaged axial velocity value corresponding to each operating condition, and the measure points are shown in figure 7 with black lines. The horizontal axis means location of radial position R normalized by the distance to the wall from center of runner rotation R_0 . In these figures, model test results are plotted in red marks and CFD results are shown in solid line and dashed line. The solid lines indicate axial direction velocity and dashed lines indicate tangential direction velocity. The minus value of axial velocity indicates the mainstream direction of flow.

1) Velocity distribution at intake

The velocity distributions at intake center cross section are shown in Figure 8. The velocity is at intake is affected by head tank and upstream rectification grid. Therefore the velocity distribution is not uniform. In particular due to the effect of rectification grid, there are low speed regions in some area and its effect is appeared most strongly in the results of the LES. Comparing the experimental results and the CFD results, since the measurement error of the experimental results is large there is large difference between the CFD results and the test results in the tangential direction.

2) Velocity distribution at guide vane outlet

The velocity distributions at guide vane outlet center cross section are shown in Figure 9. Because the guide vane outlet flow is rectified by the guide vanes, the biased flow in the left and right which occurs at the intake is hardly observed. In addition, the difference in the velocity distribution due to the difference in the CFD method is small. However, the velocity near the wall surface obtained by CFD is smaller than that of model test results.

3) Velocity distribution at runner outlet

The velocity distributions at runner outlet center cross section are shown in Figure 10. There is a large difference in the velocity distribution due to the difference in the CFD method. Comparing CFD results, although no significant difference was seen in the velocity distribution in the left side and right side except Frozen rotor method. Because the CFD applying Frozen rotor method is steady calculation and the velocity distribution at runner outlet is not averaged, therefore the runner outlet velocity distribution is affected by the position of the runner blades. The velocity distributions obtained by Stage method, SST method and DES method are almost same. However, the velocity distribution of LES is significantly different from the others. In R/R_0 is 0.8 or less, the numerical results of Stage,

SST and DES are in good agreement with the model test results. The difference of velocity distribution near the wall is large in any CFD method, but in particular the difference is large in the LES. The velocity distribution difference between the CFD and model test results is affecting the difference of the draft tube loss.

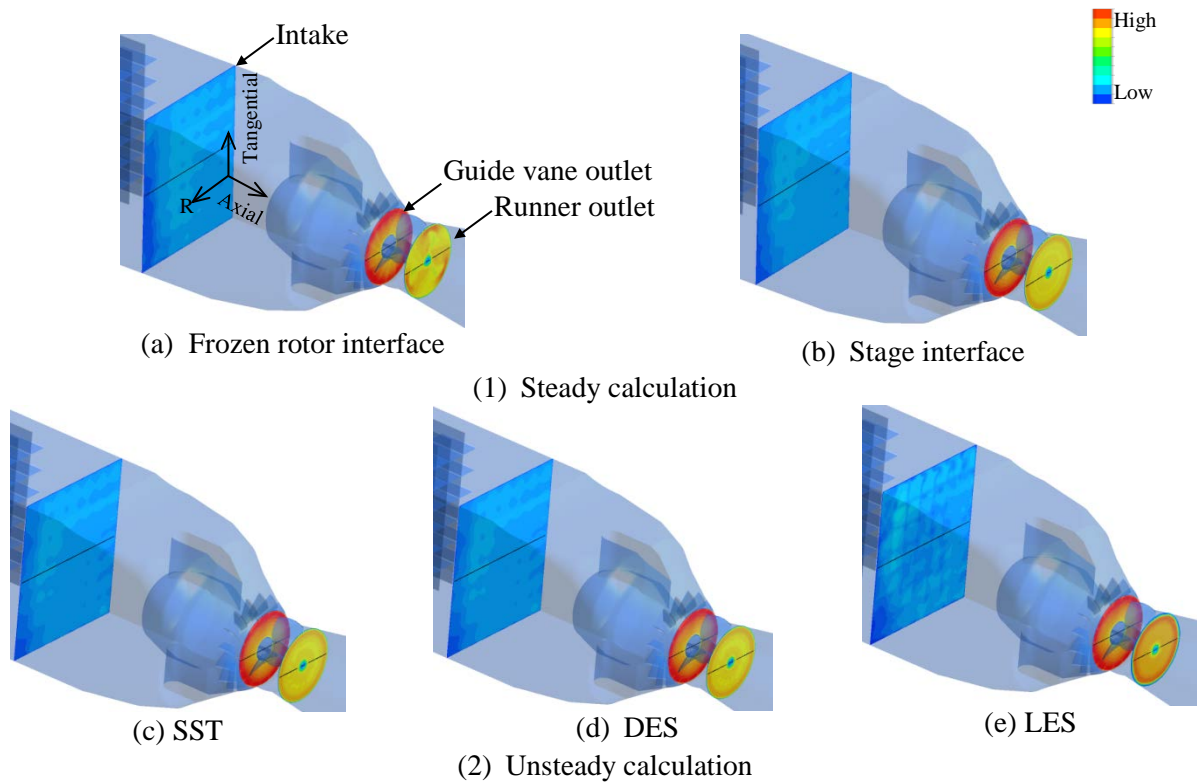


Figure 7. Flow velocity distributions at intake, guide vane outlet and runner outlet

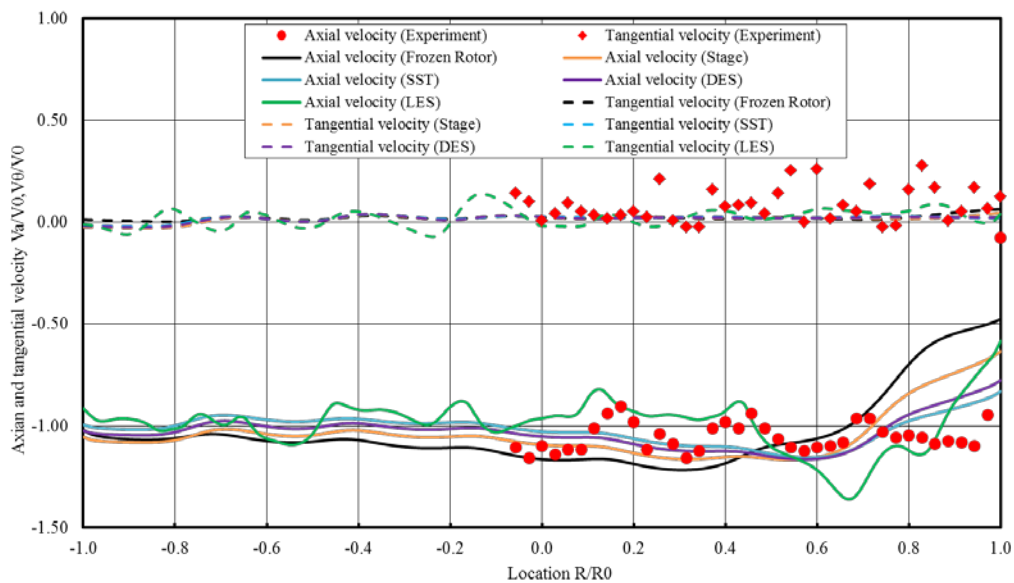


Figure 8. Flow velocity distributions numerically simulated and experimentally measured at intake

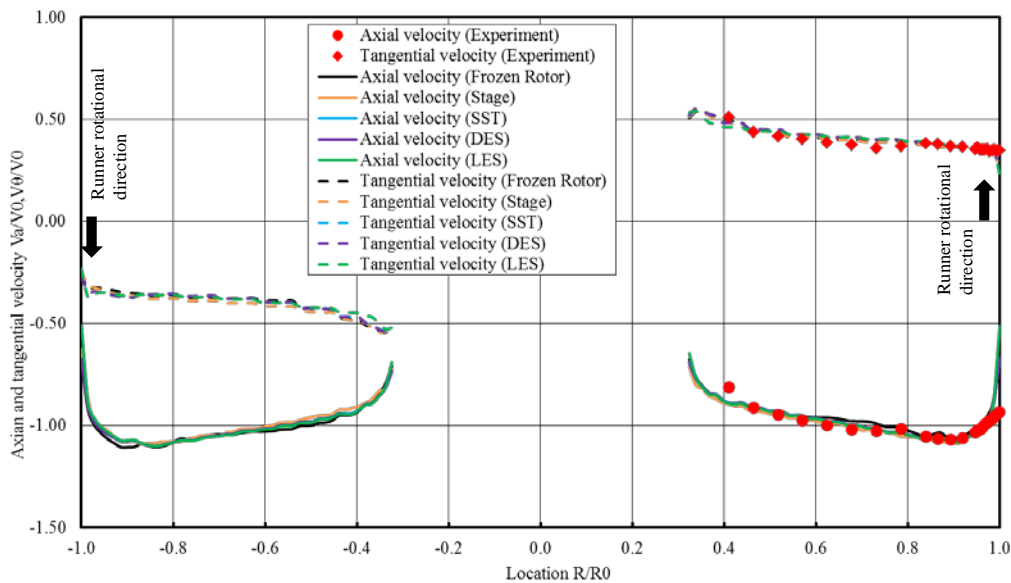


Figure 9. Flow velocity distributions numerically simulated and experimentally measured at guide vane outlet

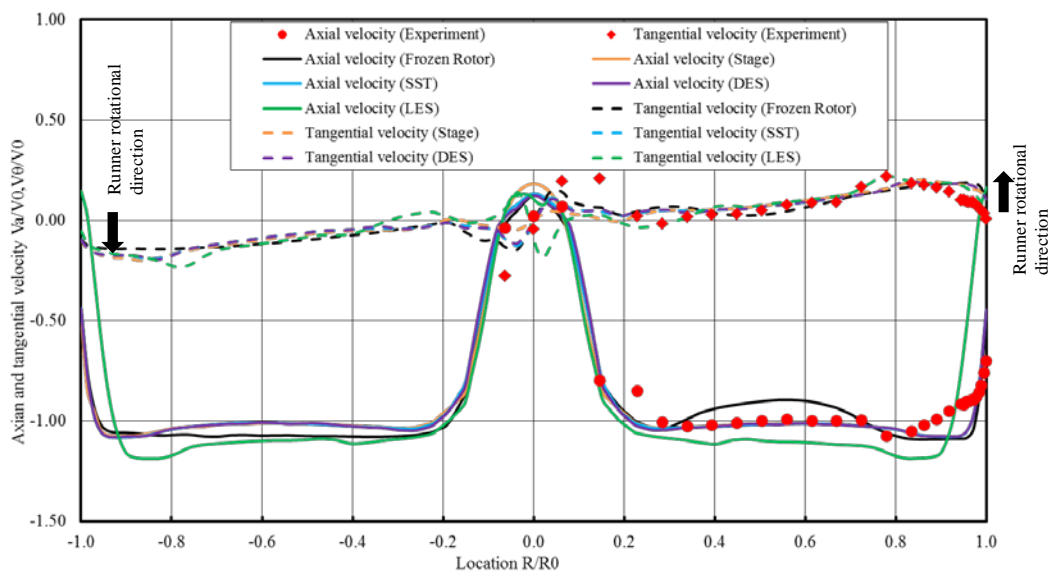


Figure 10. Flow velocity distributions numerically simulated and experimentally measured at runner outlet

4.2. Pressure fluctuation characteristic

The pressure fluctuation is recognizable by measuring the near-wall pressure inside the flow passage over a period of time. The numerical and experimental results for the pressure fluctuation characteristics are shown in Figure 11. The pressure fluctuation was experimentally measured by using the pressure transducers set on the upper draft tube wall. It is clearly that there is a huge discrepancy between the numerical and experimental data. Figure 12 shows viscosity contour. It is known that the eddy viscosity rises at the runner outlet and therefore damps out the vortex and fluctuation phenomena. As for the SST and DES calculation, the pressure fluctuation is damped out because of the increase of eddy viscosity. On the other hand, LES has resolved a relatively low eddy viscosity throughout the

flow passage. However, because of the difference of velocity distribution at draft tube between CFD and model test result, there is huge discrepancy between the LES results and experimental data.

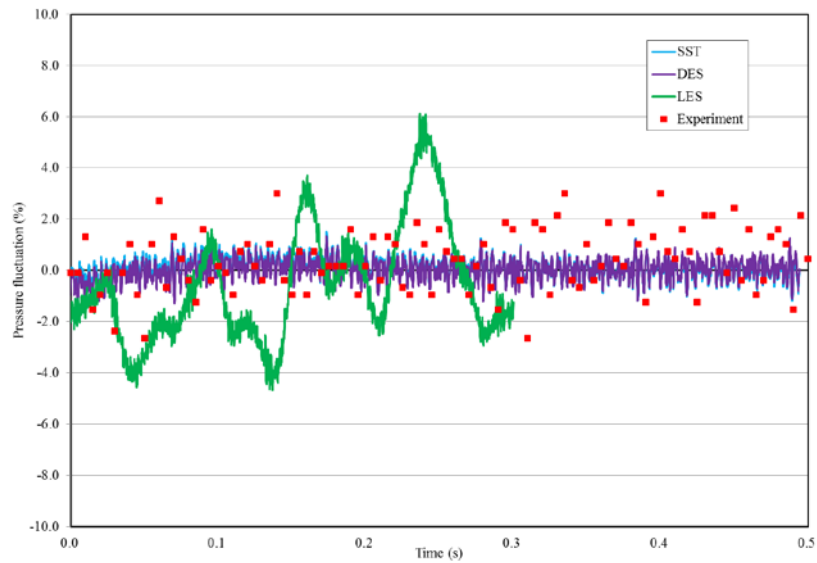


Figure 11. Runner outlet pressure fluctuation comparison between experimental and numerical results

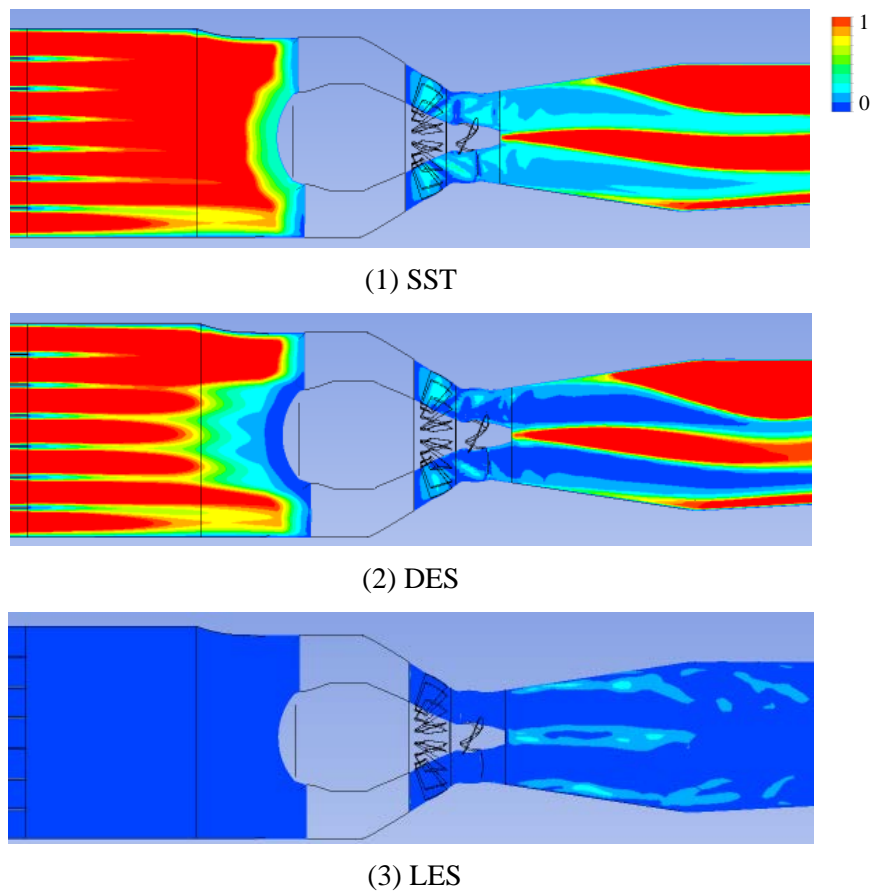


Figure 12. Eddy viscosity contour

5. Conclusions

The high accuracy prediction method based on the whole flow passage model is applied for the study of a Bulb turbine and the prediction accuracy is evaluated with RANS, LES and DES. The prediction accuracy was evaluated to compare with the model test results for efficiency characteristic and pressure fluctuation characteristic. The results obtained are as follows:

- (1) As for the efficiency characteristic near on-cam condition of a Bulb turbine is accurately captured by the proposed numerical method with SST turbulence model or DES.
- (2) As for the analysis accuracy regarding pressure fluctuation characteristic and turbine characteristics at off-cam operating condition, the proposed numerical methods are not enough. Therefore it found that there is a need to further study.

Evaluated prediction method for the turbine flow and performance is introduced to facilitate the future design and research works on Bulb type turbine.

Incidentally, the same analysis grid in any analysis technique was used in this paper. Therefore results of LES have large difference between the model test results. However we considered to be capable of high precision analysis by optimizing the analysis grid.

Acknowledgments

This work was completed by the help of the project members in hydraulic research laboratory of Toshiba Corporation and the support of members in Toshiba Information System Corporation. The authors would like to acknowledge Kiyoshi MATSUMOTO, Pohan KO and Yuusuke NAKAHARA for helpful advice.

Product names mentioned herein may be trademarks of their respective companies.

References

- [1] Enomoto. Y, et al, "Design Optimization of a High Specific Speed Francis Turbine Runner using Multi-Objective Genetic Algorithm", 23rd IAHR Symposium, Yokohama, Japan, 2006.
- [2] Kawajiri. H, et al, "Design Optimization Method for Francis Turbine" 27th IAHR Symposium, Montreal, Canada, 2014.
- [3] Shingai, K. et al, "MULTI-OBJECTIVE OPTIMIZATION OF DIAGONAL FLOWTYPE REVERSIBLE PUMP-TURBINES" Proceedings, 24th IAHR Symposium, FOZ DO IGUASSU, 2008
- [4] Kurosawa, S. et al, "Virtual Model Test for a Francis Turbine", Proceedings, 25th IAHR Symposium, Timisoara Romania, September 2010
- [5] Ko, P. et al, "Numerical simulation of turbulence flow in a Kaplan turbine -Evaluation on turbine performance prediction accuracy-" 27th IAHR Symposium, Montreal, Canada, 2014.
- [6] Kurosawa, S. et al, "Turbulent Flow Simulation for the Draft Tube of a Kaplan Turbine", Proceedings, 23rd IAHR Symposium, Yokohama Japan, October 2006